GEOLOGY | THE GEOLOGICAL SOCIETY OF AMERICA®

https://doi.org/10.1130/G46660.1

Manuscript received 6 February 2019
Revised manuscript received 19 June 2019
Manuscript accepted 25 July 2019

Published online 20 August 2019

To sink, swim, twin, or nucleate: A critical appraisal of crystal aggregation processes

Penny E. Wieser[1]*, Zoja Vukmanovic[1], Rüdiger Kilian[2], Emilie Ringe[1,3], Marian B. Holness[1], John Maclennan[1], and Marie Edmonds[1]

[1]Department of Earth Sciences, University of Cambridge, Cambridge CB2 3EQ, UK
[2]Institute for Geosciences and Geography, University Halle, 06099 Halle, Germany
[3]Department of Materials Science and Metallurgy, University of Cambridge, Cambridge CB2 3EQ, UK

ABSTRACT

Crystal aggregates in igneous rocks have been variously ascribed to growth processes (e.g., twinning, heterogeneous nucleation, epitaxial growth, dendritic growth), or dynamical processes (e.g., synneusis, accumulation during settling). We tested these hypotheses by quantifying the relative orientation of adjacent crystals using electron backscatter diffraction. Both olivine aggregates from Kīlauea volcano (Hawai'i, USA) and chromite aggregates from the Bushveld Complex (South Africa) show diverse attachment geometries inconsistent with growth processes. Near-random attachments in chromite aggregates are consistent with accumulation by settling of individual crystals. Attachment geometries and prominent geochemical differences across grain boundaries in olivine aggregates are indicative of synneusis.

INTRODUCTION

Despite the abundance of crystal aggregates in a diverse range of igneous rocks, no consensus has been reached on their origin (Schwindinger and Anderson, 1989; Jerram et al., 2003; Day and Taylor, 2007). As early as 1921, Vogt suggested that crystal aggregates form by synneusis, the "swimming together" and attachment of previously isolated crystals in a fluid medium. More recently, aggregates have been attributed to growth twinning (Welsch et al., 2013), the nucleation and growth of a daughter crystal via epitaxial growth/heterogeneous nucleation (Kirkpatrick, 1977; Dowty, 1980a; Hammer et al., 2010; Špillar and Dolejš, 2015), or the textural maturation of dendrites (Welsch et al., 2013, 2014). Previous attempts at distinguishing these hypotheses have utilized optical observations of chemical zoning (Dowty, 1980a), assessments of crystallographic orientation using a universal stage (Ross, 1957), and observations of three-dimensional (3-D) aggregate morphology (Schwindinger and Anderson, 1989; Welsch et al., 2013). In this study, we quantified changes in crystallographic orientation across grain boundaries using electron backscatter diffraction (EBSD) maps (e.g., Prior et al., 1999). This allowed direct comparison between observed aggregate geometries and those predicted by each hypothesis, even in optically isotropic or chemically homogeneous minerals. To demonstrate the versatility of this method, we investigated olivine aggregates from rapidly quenched scoria from several eruptions at Kīlauea volcano, Hawai'i, USA (A.D. ca. 1700, ca. 1920, and 1969–1975; see DR1 in the GSA Data Repository[1]; Fig. 1) and chromite crystals from the UG2 chromitite layer of the Bushveld Complex, South Africa (Fig. 2).

Unravelling the magmatic processes responsible for aggregation has important implications. At Kīlauea, olivine constitutes the principal record of pre-eruptive processes in primitive lavas. Understanding the formation and evolution of chromitite layers such as the Bushveld UG2 layer is crucial to advance our understanding of how platinum group elements are concentrated into economically viable ore deposits (Naldrett, 2013). The timing and mechanism of aggregate formation also influence crystal redistribution and accumulation in layered intrusions (Campbell, 1978; Holness et al., 2017a), and the interpretation of quantitative textural measurements such as crystal size distributions (CSDs), which frequently record kinked CSDs, and an overabundance of larger crystal sizes in volcanic rocks (Marsh, 1998).

METHODS AND RESULTS

EBSD maps were made for 93 Kīlauea aggregates (Fig. 1) and a thin section of the UG2 layer of the Bushveld Complex containing ~3500 chromite grains (Fig. 2). The crystallographic relationships between touching grains in aggregates were quantified in terms of their misorientation. This describes the coordinate transform from one crystal orientation to that across the grain boundary, displayed as an axis-angle pair (Fig. 3A). Misorientations were calculated using MTEX V5.0.4 (Bachmann et al., 2010), an open-source toolbox for MATLAB. Electron microprobe transects across olivine aggregates were obtained using a Cameca SX100 electron probe microanalyzer (EPMA; see DR1).

Olivine aggregates, consisting of 2–17 individual crystals (Fig. 1), showed misorientation axes strongly clustered about <100> (Fig. 3B), and broad peaks in misorientation angles at <5°, ~40°, and ~80° (Fig. 3C). EPMA transects across attached olivine crystals revealed flat compositional profiles in the cores of crystals, with sharp gradients across grain boundaries (Fig. 1E, sections X-X′ and Z-Z′). The distribution of chromite misorientation angles was very close to the theoretical random distribution (Fig. 4C), with the only prominent peak at 60°. Chromite misorientation axes exhibited weak clustering about <111> and <011> (Fig. 4A). Removal of the {111} twins responsible for the 60° peak resulted in a nearly uniform distribution of misorientation axes and angles (Figs. 4B and 4C).

*E-mail: pew26@cam.ac.uk.

[1]GSA Data Repository item 2019336, detailed descriptions of sample locations, sample preparation, analytical methods, EBSD data processing, and surface energy calculations, and data for electron microprobe transects, is available online at http://www.geosociety.org/datarepository/2019/, or on request from editing@geosociety.org.

CITATION: Wieser, P.E., et al., 2019, To sink, swim, twin, or nucleate: A critical appraisal of crystal aggregation processes: Geology, v. 47, p. 948–952, https://doi.org/10.1130/G46660.1

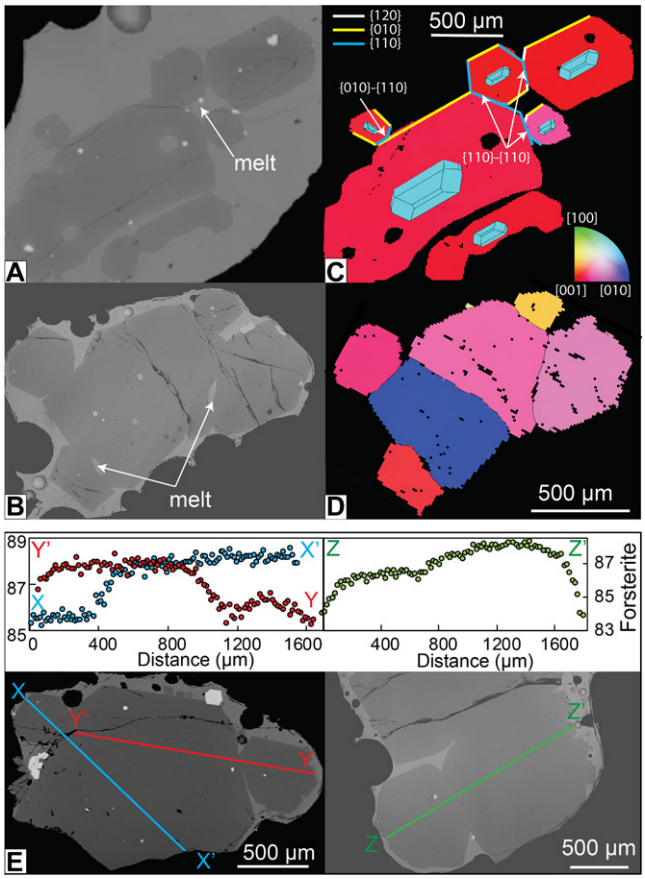

Figure 1. (A–B) Backscatter electron (BSE) images of olivine aggregates consisting of 3–5 crystals. Prominent areas of melt are trapped between neighboring crystals. (C–D) Electron backscatter diffraction (EBSD)–derived inverse pole figure maps (IPF) of aggregates, with color coding of crystal direction parallel to *Z*/image normal. For example, crystals in C are colored red to demonstrate that their <001> axes are close to vertical. Olivine shapes in C were computed using the crystalShape MTEX class (Enderlein, 1997; https://mtex-toolbox.github.io/files/doc/crystalShape_index.html), allowing assessment of facial attachments. In this case, crystals are predominantly attached along {110}-{110} faces. Note the presence of a misaligned crystal in C within an aggregate mostly formed of crystals with similar orientations. If this aggregate formed by dendritic growth, synneusis would also have to be operating. The more parsimonious explanation is that attached crystals with both high and low misorientations formed by synneusis. (E) BSE images of two olivine aggregates, showing locations of electron probe microanalyzer transects. Attached grains show different forsterite contents [Fo = 100 × Mg/(Mg + Fe), atomic]. The presence of flat plateaus within profiles X-X′ and Z-Z′ demonstrates that these transects cut across grain cores, which must have grown in different conditions. These profiles are not consistent with a scenario whereby compositionally homogeneous aggregates (formed by growth processes) were altered by diffusion or late-stage growth. The presence of steep gradients in forsterite content between crystals indicates that limited diffusive re-equilibration occurred following aggregation.

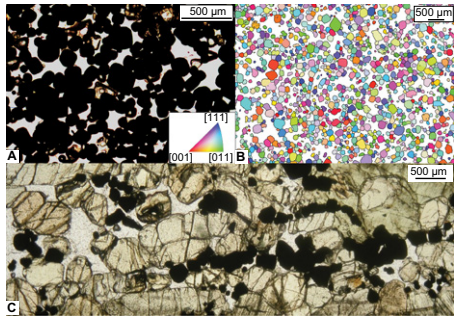

Figure 2. (A) Transmitted light image of a small region of the UG2 chromitite (Bushveld Complex, South Africa) thin section. Chromites (black) form a prominent touching network. (B) Electron backscatter diffraction (EBSD)–derived inverse pole figure (IPF) map of larger area of thin section, color coded as in Figure 1 (e.g., grains with their <111> axes vertical appear blue). The wide range of colors points to an absence of crystallographic preferred orientation. (C) Transmitted light image of a chromite-poor pyroxenite, lying 0.5 m above UG2 chromitite layer. Touching frameworks of chromite crystals are relatively scarce compared to chromitite layer itself (A and B), and separated and attached chromite crystals rest on underlying pyroxene grains. This indicates that chromites settle as isolated grains (accounting for their random orientations), with aggregates only forming when sufficient grains settled in one place.

Physical Aggregation of Crystals

Hydrodynamic processes within magmatic systems can drive the aggregation of preformed crystals (McIntire et al., 2019). One such process is synneusis (Vogt, 1921; Vance, 1969). While the driving forces associated with interfacial energy minimization during synneusis are too localized to drive crystals together (Dowty, 1980a), crystals may be aligned while suspended in convecting magma (Holness et al., 2017b), or during settling (Schwindinger and Anderson, 1989; Schwindinger, 1999), resulting in their attachment in specific orientations. Once sufficiently close, reductions in interfacial energy associated with particular crystallographic orientations can drive small readjustments in aggregate geometry (Dowty, 1980a), before further crystal growth cements the crystals together.

To assess the synneusis hypothesis in Kīlauea olivine aggregates, the faces of attachment between adjacent crystals were assessed by superimposing 3-D olivine shapes onto EBSD maps using the crystalShape MTEX class (Enderlein, 1997; https://mtex-toolbox.github.io/files/doc/crystalShape_index.html; Fig. 1C), and these were compared to the predicted hydrodynamical alignments during settling. Oblate olivines align their axis of symmetry vertically during settling, while prolate olivines align their axis of symmetry horizontally (Leal, 1980). This creates mostly {010} attachments in oblate olivines, and {110} attachments in prolate olivines, with occasional {021} attachments in both cases (Schwindinger and Anderson, 1989). We anticipate that similar alignments would also occur during convection.

The {110}-{110} attachments were the most commonly observed geometry in Kīlauea aggregates (Fig. 1C), followed by {010}-{010} or parallel {021}-{021} attachments (difficult to distinguish in two dimensions). Crystals that are perfectly attached along parallel {110}-{110}, {010}-{010} and {021}-{021} faces would have identical orientations, while perfect attachments along {021}-{010} and perpendicular {021}-{021} faces would generate misorientations about <100> of 40.4° and 80.9°, respectively. The presence of broad misorientation angle peaks centered about these angles is strong evidence for synneusis (Fig. 3C). Unlike crystal growth processes, which favor specific crystallographic relationships, attachment by synneusis can easily generate misalignments from these ideal attachment geometries through the mechanical hindrance to reorientation driven by the reduction of interfacial energies (Vance, 1969; Nespolo and Ferraris, 2004), or near-random attachment under conditions of high supersaturation (Schwindinger and Anderson, 1989). Imperfect attachment by synneusis also accounts for the presence of discontinuous melt films between adjacent olivine crystals (Figs. 1A and 1B). If formed during growth, such films would impose high energy penalties.

Finally, the EPMA transects support the hypothesis that the olivine aggregates formed by synneusis (Fig. 1E). While synneusis can bring together crystals with different core compositions that formed in disparate environments (Schwindinger and Anderson, 1989), aggregates produced by twinning or dendritic growth share a common history, so the cores of attached crystals should have identical chemistry (Philpotts et al., 1998). The sharp gradients in forsterite contents (which dissipates rapidly by diffusion) suggest that the aggregation event occurred shortly before eruption. Crystal aggregation may occur following a disturbance to the magmatic system, triggering their eruption, or during transport of the magma to the eruption site.

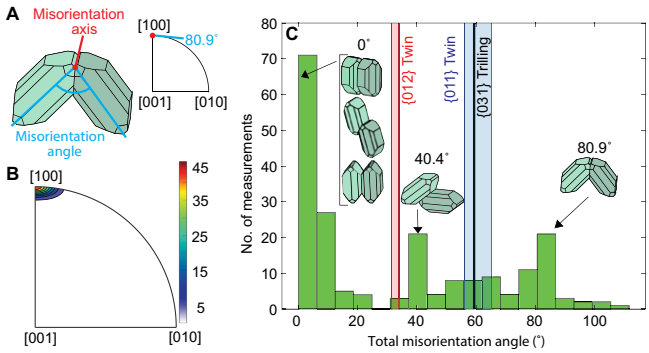

Figure 3. (A) Schematic diagram showing the misorientation angle (80.9°) and axis (<100>) for a hypothetical olivine aggregate. (B–C) Misorientation axes and angles for 203 touching olivine crystals within 93 aggregates. Misorientation axes cluster strongly at <100>. Misorientation angles exhibit prominent peaks around angles predicted for perfect attachment along different crystal faces (crystal aggregates drawn in SHAPE7.4; Dowty, 1980b). Small peaks close to {011} and {012} twin laws are also present. Color scale shown in B has units of 'multiples of uniform distribution'.

Evaluating the role of physical aggregation in the formation of chromite aggregates is complicated because attachment along the only crystal face, {111}, produces misorientation axes indistinguishable from primary twinning (60° rotation about <111>; Deer, 1966). However, this geometric relationship is relatively uncommon, and the removal of misorientations corresponding to the chromite twin law (and effects induced by crystal symmetry) produces a near-uniform misorientation axis distribution, and an angle distribution resembling the theoretical random distribution (Figs. 4B and 4C). This implies that chromite grains are randomly aggregated by a mechanism that is not selective to crystallographic orientation; this is inconsistent with the attachment of {111} faces by synneusis, or various growth processes. We suggest that the randomly oriented touching frameworks of chromite grains formed during the settling of individual grains through the overlying magma column to the top of the cumulate pile (Jackson, 1961). This hypothesis is consistent with microstructures in the cumulates overlying UG2, in which individual chromite grains apparently rest on underlying pyroxene primocrysts (Fig. 2C).

Crystal Growth Processes

Crystal aggregates attached along specific planes have also been attributed to primary twinning (Welsch et al., 2013). However, neighboring chromite grains displaying twin relations are relatively rare (<10% of neighboring grains, based on deviations from ideal twin laws; Brandon, 1966; see DR1). Similarly, <7% of neighboring olivines are related by the three olivine twin laws (twinning on {011}, {012}, and {031}, corresponding to misorientations about <100> of 60.7°, 32.6°, and 59.3°, respectively; Dodd and Calef, 1971; Azevedo and Nespolo, 2017). Thus, twinning was not the dominant cause of grain aggregation in our samples.

Dowty (1980a) suggested that the textural and chemical characteristics of crystal aggregates could result from epitaxial growth or heterogeneous nucleation. These processes, driven by the reduction of the activation barrier to nucleation by the presence of an existing crystalline substrate in the melt (Lofgren, 1983; Mithen and Sear, 2014), are well documented in multiphase aggregates (Kirkpatrick, 1977; Hammer et al., 2010). However, in monomineralic aggregates, nucleation and growth of a daughter crystal are associated with energy penalties. The increased surface area per unit volume (and increased interfacial energy) caused by the growth of a daughter crystal was assessed by comparing an individual crystal of a given volume with an aggregate with the same total volume composed of two identical crystals (volumes and areas calculated in SHAPE7.4; Dowty, 1980b; see DR1). As chromite crystals express only {111} faces, the increase in interfacial energy for aggregates compared to individual crystals (11%) is independent of the interfacial energy of the {111} face. For olivine, theoretical surface energies for the six different olivine faces in a vacuum at 0 K (Bruno et al., 2014) were used. Regardless of the attachment face, the growth of a daughter crystal in olivine is accompanied by significant energy penalties (13%–24%; see DR1).

Energy penalties for heterogenous nucleation are even greater. While epitaxial growth describes the nucleation of crystals in a specific crystallographic orientation with respect to the host crystal (identical or twin orientations in single-phase aggregates; Mithen and Sear, 2014), heterogeneous nucleation has no such orientation constraints. The large lattice mismatches, and associated energy penalties, generated by heterogeneous nucleation may drive the detachment of a poorly orientated unit, followed by reattachment in a more-favorable orientation (Buerger, 1945). In certain cases, it may even be more energetically favorable for the components of the misaligned daughter crystal to remain in the liquid state (Brugger and Hammer, 2015).

The larger energy penalties for heterogeneous nucleation compared to epitaxial growth, alongside lower nucleation rates for mismatching parent and daughter lattices (Turnbull and Vonnegut, 1952), mean that heterogeneous nucleation should occur less frequently than epitaxy in monomineralic aggregates. Olivine and chromite aggregates show little evidence for epitaxy; twin relationships are rare (Figs. 3 and 4), and no crystals with uniform orientations show external morphologies indicative of aggregation. Given the limited evidence for epitaxial growth, it is improbable that the energetically unfavorable process of heterogeneous nucleation was the dominant cause of grain aggregation in this study.

Welsch et al. (2013) proposed that polyhedral aggregates are produced during an early period of dendritic growth, followed by textural ripening. This hypothesis was based on observations that attached olivine crystals have identical orientations, are in continuous contact, and are superimposed into chains of decreasing crystal size elongated along <100> (Welsch et al., 2013). However, crystallographic branching in dendrites (Cody and Cody, 1995; Faure et al., 2003a, 2003b) is associated with misorientations lower than ~3° (Faure et al., 2003b), and so it cannot account for the 86% of olivine aggregates with misorientations >3° (Fig. 3). Additionally, neighboring crystals in the subset of olivine aggregates displaying small misorientations (<5°) were often separated by pockets of melt, and they showed no preferential elongation direction or size ordering (Fig. 1A). While the textural maturation of noncrystallographic branching dendrites (Keith and Padden, 1963; Donaldson, 1976) could produce the 86% of aggregates with

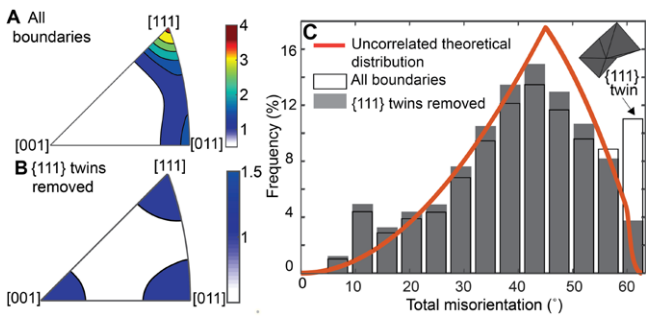

Figure 4. (A) Chromite misorientation axes show moderate clustering about <111> (for ~3500 chromite grains within one thin section). (B) Removal of {111} twins and normalization to theoretical axis distribution (see DR1 [see text footnote 1]) leave a near-uniform axis distribution. (C) Chromite aggregates show a wide range of misorientation angles. Removal of the prominent peak at 60° caused by {111} twins results in a distribution similar to the symmetry-induced distribution. Color scale shown in B has units of 'multiples of uniform distribution'.

large misorientation angles, the crystallographic signatures of branching olivine dendrites from West Greenland picrites differ from those of olivine aggregates (Larsen and Pedersen, 2000; Fig. DR5). While olivine dendrites and aggregates both display a misorientation angle peak at <20°, dendrites show no peaks at higher angles (Fig. DR5). The differences between these distributions are statistically significant ($p = 0.013$; Kolmogorov-Smirnov test). Additionally, misorientation axes in branching dendrites form a bimodal distribution, with a primary maximum at <010> (Donaldson, 1976) and a minor secondary maximum at <100> (Fig. DR5). This contrasts with the strong clustering of olivine misorientation axes at <100> in Kīlauea aggregates (Fig. 3B). Overall, the crystallographic and textural signatures of olivine aggregation are inconsistent with an origin from noncrystallographic branching during dendritic growth.

CONCLUSIONS

The large range of misorientations in chromite and olivine aggregates cannot be explained by crystal growth processes, which favor specific crystallographic relationships. Observed facial attachments and compositional profiles across adjacent olivines are consistent with crystal aggregation by synneusis shortly before eruption. In crystal populations affected by synneusis, textural investigations such as crystal size distributions must be constructed from measurements of individual grains within an aggregate. Consideration of the total size of an aggregate is only justified if aggregation can be attributed to twinning or dendritic growth. To distinguish between these cases routinely, a workflow could be developed whereby the origin of grain aggregation is assessed by EBSD maps, which are subsequently used to generate "informed" CSDs. The random crystallographic relationships between adjacent chromite grains in our sample of the UG2 chromitite layer are best explained by the formation of touching networks following crystal settling. Settling as individual crystals rather than aggregates has implications for initial mush porosity and accumulation time scales, with relevance to the formation of economically viable platinum group element deposits.

ACKNOWLEDGMENTS

We thank Giulio Lampronti and Iris Buisman for help with collecting and interpreting electron backscatter diffraction and electron probe microanalyzer data, and Eric Dowty for providing guidance on the use of SHAPE software. Isobel Sides (funded by a Natural Environment Research Council [NERC] studentship) and Don Swanson (U.S. Geological Survey) collected the Kīlauea scoria samples. Lotte Larsen and Ilya Veksler are thanked for providing the Greenland picrites and UG2 chromitite samples, respectively. We thank Chris Clark for editorial handling, and François Faure, Dougal Jerram, and one anonymous reviewer for their constructive comments, which helped to greatly improve this manuscript. Wieser was funded by NERC doctoral training partnership (DTP) studentship NE/L002507/1; Vukmanovic was funded by Marie Curie grant 708131-EFOX-H2020-MSCA-IF-2015.

REFERENCES CITED

Azevedo, S., and Nespolo, M., 2017, Twinning in olivine group revisited: European Journal of Mineralogy, v. 29, p. 213–226, https://doi.org/10.1127/ejm/2017/0029-2598.

Bachmann, F., Hielscher, R., and Schaeben, H., 2010, Texture analysis with MTEX—Free and open source software toolbox, *in* Klein, H., and Schwarzer, R.A., eds., Texture and Anisotropy of Polycrystals III: Trans Tech Publications Solid State Phenomena Volume 160, p. 63–68, https://doi.org/10.4028/www.scientific.net/SSP.160.63.

Brandon, D.G., 1966, The structure of high-angle grain boundaries: Acta Metallurgica, v. 14, p. 1479–1484, https://doi.org/10.1016/0001-6160(66)90168-4.

Brugger, C.R., and Hammer, J.E., 2015, Prevalence of growth twins among anhedral plagioclase microlites: The American Mineralogist, v. 100, p. 385–395, https://doi.org/10.2138/am-2015-4809.

Bruno, M., Massaro, F.R., Prencipe, M., Demichelis, R., De La Pierre, M., and Nestola, F., 2014, Ab initio calculations of the main crystal surfaces of forsterite (Mg_2SiO_4): A preliminary study to understand the nature of geochemical processes at the olivine interface: The Journal of Physical Chemistry C, v. 118, p. 2498–2506, https://doi.org/10.1021/jp409837d.

Buerger, M.J., 1945, The genesis of twin crystals: American Mineralogist, v. 30, p. 469–482.

Campbell, I., 1978, Some problems with the cumulus theory: Lithos, v. 11, p. 311–323, https://doi.org/10.1016/0024-4937(78)90038-5.

Cody, A.M., and Cody, R.D., 1995, Dendrite formation by apparent repeated twinning of calcium oxalate dihydrate: Journal of Crystal Growth, v. 151, p. 369–374, https://doi.org/10.1016/0022-0248(94)00964-3.

Day, J.M., and Taylor, L.A., 2007, On the structure of mare basalt lava flows from textural analysis of the LaPaz Icefield and Northwest Africa 032 lunar meteorites: Meteoritics & Planetary Science, v. 42, p. 3–17, https://doi.org/10.1111/j.1945-5100.2007.tb00213.x.

Deer, W.A., 1966, An Introduction to the Rock-Forming Minerals: London, Longman, 528 p.

Dodd, R.T., and Calef, C., 1971, Twinning and intergrowth of olivine crystals in chondritic meteorites: Mineralogical Magazine, v. 38, p. 324–327, https://doi.org/10.1180/minmag.1971.038.295.06.

Donaldson, C.H., 1976, An experimental investigation of olivine morphology: Contributions to Mineralogy and Petrology, v. 57, p. 187–213, https://doi.org/10.1007/BF00405225.

Dowty, E., 1980a, Synneusis reconsidered: Contributions to Mineralogy and Petrology, v. 74, p. 75–84, https://doi.org/10.1007/BF00375491.

Dowty, E., 1980b, Computing and drawing crystal shapes: The American Mineralogist, v. 65, p. 465–471.

Enderlein, J., 1997, A package for displaying crystal morphology: Mathematica Journal, v. 7, https://www.mathematica-journal.com/issue/v7i1/article/enderlein/index.html.

Faure, F., Trolliard, G., Nicollet, C., and Montel, J.M., 2003a, A developmental model of olivine morphology as a function of the cooling rate and the degree of undercooling: Contributions to Mineralogy and Petrology, v. 145, p. 251–263, https://doi.org/10.1007/s00410-003-0449-y.

Faure, F., Trolliard, G., and Soulestin, B., 2003b, TEM investigation of forsterite dendrites: The American Mineralogist, v. 88, p. 1241–1250 https://doi.org/10.2138/am-2003-8-907.

Hammer, J.E., Sharp, T.G., and Wessel, P., 2010, Heterogeneous nucleation and epitaxial crystal growth of magmatic minerals: Geology, v. 38, p. 367–370, https://doi.org/10.1130/G30601.1.

Holness, M.B., Vukmanovic, Z., and Mariani, E., 2017a, Assessing the role of compaction in the formation of adcumulates: A microstructural perspective: Journal of Petrology, v. 58, p. 643–673, https://doi.org/10.1093/petrology/egx037.

Holness, M.B., Farr, R., and Neufeld, J.A., 2017b, Crystal settling and convection in the Shaint Isles main sill: Contributions to Mineralogy and Petrology, v. 172, p. 7, https://doi.org/10.1007/s00410-016-1325-x.

Jackson, E.D., 1961, Primary Textures and Mineral Associations in the Ultramafic Zone of the Stillwater Complex Montana: The Petrographic Features and Origin of the Layered Chromitites, Bronzitites, and Harzburgites in the Lower Part of the Stillwater Complex: Washington, D.C., U.S. Government Printing Office, 106 p., https://doi.org/10.3133/pp358.

Jerram, D.A., Cheadle, M.J., and Philpotts, A.R., 2003, Quantifying the building blocks of igneous rocks: Are clustered crystal frameworks the foundation?: Journal of Petrology, v. 44, p. 2033–2051, https://doi.org/10.1093/petrology/egg069.

Keith, H.D., and Padden, F.J., Jr., 1963, A phenomenological theory of spherulitic crystallization: Journal of Applied Physics, v. 34, p. 2409–2421, https://doi.org/10.1063/1.1702757.

Kirkpatrick, R.J., 1977, Nucleation and growth of plagioclase, Makaopuhi and Alae lava lakes, Kilauea Volcano, Hawaii: Geological Society of America Bulletin, v. 88, p. 78–84, https://doi.org/10.1130/0016-7606(1977)88<78:NAGOPM>2.0.CO;2.

Larsen, L.M., and Pedersen, A.K., 2000, Processes in high-Mg, high-T magmas: Evidence from olivine, chromite and glass in Palaeogene picrites from West Greenland: Journal of Petrology, v. 41, p. 1071–1098, https://doi.org/10.1093/petrology/41.7.1071.

Leal, L.G., 1980, Particle motions in a viscous fluid: Annual Review of Fluid Mechanics, v. 12, p. 435–476, https://doi.org/10.1146/annurev.fl.12.010180.002251.

Lofgren, G.E., 1983, Effect of heterogeneous nucleation on basaltic textures: A dynamic crystallization study: Journal of Petrology, v. 24, p. 229–255, https://doi.org/10.1093/petrology/24.3.229.

Marsh, B.D., 1998, On the interpretation of crystal size distributions in magmatic systems: Journal of Petrology, v. 39, p. 553–599, https://doi.org/10.1093/petroj/39.4.553.

McIntire, M.Z., Bergantz, G.W., and Schleicher, J.M., 2019, On the hydrodynamics of crystal clustering: Philosophical Transactions of the Royal Society, ser. A, v. 377, https://doi.org/10.1098/rsta.2018.0015.

Mithen, J.P., and Sear, R.P., 2014, Epitaxial nucleation of a crystal on a crystalline surface: EPL (Europhysics Letters), v. 105, p. 18004, https://doi.org/10.1209/0295-5075/105/18004.

Naldrett, A.J., 2013, Magmatic Sulfide Deposits: Geology, Geochemistry and Exploration: Berlin, Springer Science & Business Media, 727 p.

Nespolo, M., and Ferraris, G., 2004, The oriented attachment mechanism in the formation of twins—A survey: European Journal of Mineralogy, v. 16, p. 401–406, https://doi.org/10.1127/0935-1221/2004/0016-0401.

Philpotts, A.R., Shi, J., and Brustman, C., 1998, Role of plagioclase crystal chains in the differentiation

of partly crystallized basaltic magma: Nature, v. 395, p. 343, https://doi.org/10.1038/26404.
Prior, D.J., et al., 1999, The application of electron backscatter diffraction and orientation contrast imaging in the SEM to textural problems in rocks: The American Mineralogist, v. 84, p. 1741–1759, https://doi.org/10.2138/am-1999-11-1204.
Ross, J.V., 1957, Combination twinning in plagioclase felspars: American Journal of Science, v. 255, p. 650–655, https://doi.org/10.2475/ajs.255.9.650.
Schwindinger, K.R., 1999, Particle dynamics and aggregation of crystals in a magma chamber with application to Kilauea Iki olivines: Journal of Volcanology and Geothermal Research, v. 88, p. 209–238, https://doi.org/10.1016/S0377-0273(99)00009-8.
Schwindinger, K.R., and Anderson, A.T., 1989, Synneusis of Kilauea Iki olivines: Contributions to Mineralogy and Petrology, v. 103, p. 187–198, https://doi.org/10.1007/BF00378504.
Špillar, V., and Dolejš, D., 2015, Heterogeneous nucleation as the predominant mode of crystallization in natural magmas: Numerical model and implications for crystal-melt interaction: Contributions to Mineralogy and Petrology, v. 169, p. 4, https://doi.org/10.1007/s00410-014-1103-6.
Turnbull, D., and Vonnegut, B., 1952, Nucleation catalysis: Industrial & Engineering Chemistry, v. 44, p. 1292–1298, https://doi.org/10.1021/ie50510a031.
Vance, J.A., 1969, On synneusis: Contributions to Mineralogy and Petrology, v. 24, p. 7–29, https://doi.org/10.1007/BF00398750.
Vogt, J.H.L., 1921, The physical chemistry of the crystallization and magmatic differentiation of igneous rocks: The Journal of Geology, v. 29, p. 318–350, https://doi.org/10.1086/622785.
Welsch, B., Faure, F., Famin, V., Baronnet, A., and Bachèlery, P., 2013, Dendritic crystallization: A single process for all the textures of olivine in basalts?: Journal of Petrology, v. 54, p. 539–574, https://doi.org/10.1093/petrology/egs077.
Welsch, B., Hammer, J., and Hellebrand, E., 2014, Phosphorus zoning reveals dendritic architecture of olivine: Geology, v. 42, p. 867–870, https://doi.org/10.1130/G35691.1.

Printed in USA